INORGANIC CHEMISTRY FRONTIERS

RESEARCH ARTICLE

View Article Online
View Journal | View Issue

Cite this: *Inorg. Chem. Front.*, 2025, **12**, 7752

Symmetry breaking of rare earth Eu(III) complexes with an achiral aromatic ligand: achieving strong emission and ultra-narrowband circularly polarized luminescence

Zhi Chen, †[a] Wenmin Xu,†[a] Chunhua Hu,[a] Zhen Liu,[a] Suwen Lin,[a] Shaomeng Guo,[b,c] Zhupin Chen,[a] Mianling Huang,[a] Zhen-Qiang Yu,[a] Wei-Hong Zhu[b,c] and Yue Wu*[a]

Received 10th June 2025,
Accepted 11th August 2025

DOI: 10.1039/d5qi01288k

rsc.li/frontiers-inorganic

Narrowband circularly polarized luminescence (CPL) plays a critical role in fabricating high color purity displays but is still in its infancy. Given the unique f–f transition of electrons in the 4f orbital, rare earth complexes generally possess very narrowband emission. However, most of the chiral Eu(III) complexes exhibit weak emission due to the limited light harvesting (absorption) ability of stereoscopic but non-aromatic ligands. Herein, achiral 1-(2-naphthoyl)-3,3,3-trifluoroacetone (NTA), including π-conjugated naphthalene and β-diketone, as a coordinating moiety is employed to coordinate with Eu(III) to achieve the metal–organic complex **EuNTA**. Benefiting from its immense absorption (ε = 88 500 M^{-1} cm^{-1}), the luminescence quantum yield of **EuNTA** is as high as 91%. Due to the strong intermolecular π–π and C–H···π interactions, purely chiral aggregates of symmetry breaking-induced **Λ-EuNTA** and **Δ-EuNTA** have been successfully obtained through crystallization with spontaneous resolution, resulting in highly asymmetric CPL with a dissymmetry factor of 10^{-2}. Impressively, **Λ/Δ-EuNTA** exhibits extremely narrowband CPL with a full width at half maximum of mere 5 nm. Such an achiral π-conjugated ligand-induced symmetry breaking strategy can achieve both strong emission and ultra-narrowband CPL, which is anticipated to put forward a new route toward the further utilization of rare earth complexes in advanced display technology.

Introduction

Circularly polarized luminescence (CPL), as a kind of excited-state chirality, could be an ideal descriptor of chiroptical activities.[1–3] Until now, CPL has received wide attention because CPL exhibits left- or right-handed luminescence, which can be regarded as part of a high-level visual perception for supplying one more dimension of information compared to conventional luminescence.[3–5] Thus, developing chiroptical functional materials with CPL plays a pivotal role in three-dimensional displays,[5,6] information encryption,[7–9] and polarization-based bioimaging.[10] To realize high-contrast displays, the International Telecommunication Union announced a color purity standard in 2012,[11] and a small full width at half-maximum (FWHM) becomes a crucial parameter to evaluate the performance of CPL materials. Nevertheless, most CPL materials suffer from broadband emission with a large FWHM of >60 nm due to their intrinsic vibronic coupling between their ground and excited states.[12–15] Therefore, achieving narrowband CPL with a small FWHM is still an unsolved issue and considered as the bottleneck for further advancing CPL application.

Given the unique f–f transition of electrons in the 4f orbital, rare earth complexes generally possess very narrowband emission (FWHM ≤ 10 nm),[16–20] which makes chiral rare earth complexes with high color purity CPL as ideal candidates for high-contrast displays. Therefore, chiral ligands have been widely employed to coordinate with lanthanide (Ln) metal ions to construct chiral Ln complexes, especially for chiral Eu(III) complexes with narrowband CPL and a high dissymmetry

[a]*College of Chemistry and Environmental Engineering, Shenzhen University, Shenzhen 518060, China. E-mail: wuyue@szu.edu.cn*
[b]*Key Laboratory for Advanced Materials and Institute of Fine Chemicals, Joint International Research Laboratory of Precision Chemistry and Molecular Engineering, Feringa Nobel Prize Scientist Joint Research Center, Frontiers Science Center for Materiobiology and Dynamic Chemistry, School of Chemistry and Molecular Engineering, East China University of Science and Technology, Shanghai 200237, China*
[c]*Center of Photosensitive Chemicals Engineering, School of Chemistry and Molecular Engineering, East China University of Science and Technology, Shanghai 200237, China*
†These authors contributed equally to this work.

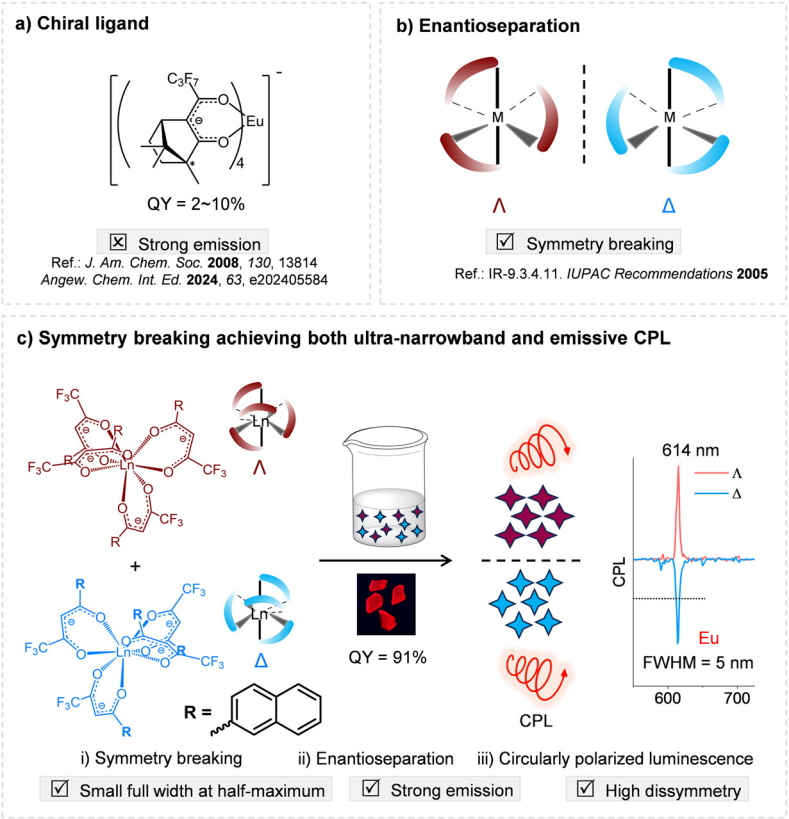

Fig. 1 Eu(III) complex with an achiral aromatic ligand for narrowband and emissive CPL. (a) Chiral Eu(III) complex with weak luminescence formed by a chiral ligand. (b) Λ- and Δ-enantiomers with an achiral ligand obtained through symmetry breaking and enantioseparation. (c) Λ- and Δ-enantiomers of axial chiral Ln compounds with achiral bidentate ligands (β-diketone derivative and NTA) and the schematic representation of forming conglomerates with symmetry breaking and spontaneous resolution through π–π interaction and C–H···π interaction, achieving both ultra-narrowband and strong-emission CPL.

factor (*g* value).[21–29] However, most of the chiral Eu(III) complexes exhibit weak emission with low quantum yields (QYs) due to their limited light harvesting ability (absorption) resulting from non-aromatic structures (Fig. 1a)[30–33] or low energy matching.[29] Thus, there is an urgent demand to overcome the dilemma between stereostructures for strong chirality and π-conjugated structures for light harvesting. Accordingly, it is rather significant to develop a new strategy capable of providing both strong emission and ultra-narrowband CPL.

Inspired by symmetry breaking in supramolecular assembly through an achiral building block,[34–37] C_3-symmetric monomers self-assembling into helical orientations[38,39] and coordination complexes with propeller chirality[36,40] have been reported extensively (Fig. 1b). Herein, achiral 1-(2-naphthoyl)-3,3,3-trifluoroacetone (NTA), including π-conjugated naphthalene and β-diketone, is employed as a coordination moiety to chelate with Ln(III) to construct a series of complexes (TEA)[Ln(NTA)$_4$] (Ln = Sm, Eu, Tb, Dy, and Yb; TEA = tetraethylammonium) (Fig. 1c). Although NTA as an antenna effect ligand has been widely used in lanthanide luminescent materials,[41,42] its possible chiral properties have not been explored.[43] Benefiting from intermolecular strong π–π and C–H···π interactions, enantiopure **Λ-LnNTA** and **Δ-LnNTA** have been successfully obtained as conglomerates without using any chiral reagent or chiral column through crystallization with spontaneous resolution, demonstrating high-dissymmetry left- or right-handed CPL, respectively. With the enhancement of structural aromatic degree using naphthalene, the light harvesting ability *via* absorption has been improved significantly, resulting in highly emissive luminescence accordingly. By virtue of this complex and chiral separation strategy, rare earth complexes such as **Λ-EuNTA** and **Δ-EuNTA** enable narrowband, emissive, and high-dissymmetry CPL with the following luminescence features: (i) FWHM of 5 nm, (ii) QY of 91%, and (iii) dissymmetry factor of 10^{-2}. This approach provides a general strategy for overcoming the main dilemma: high luminescence dissymmetry always suffers from suppression of emission efficiency, providing a *de novo* strategy for building CPL-active materials with striking chiroptical characteristics in color purity, luminescence quantum yield, and dissymmetry factor.

Results and discussion

Five mononuclear lanthanide complexes, **LnNTA** (where Ln = Sm, Eu, Tb, Dy, and Yb), were synthesized by heating a mixture

of 1-(2-naphthoyl)-3,3,3-trifluoroacetone (NTA), tetraethylammonium (TEA) hydroxide, and $LnCl_3$ in ethanol at 333 K. The structures of all five complexes were unambiguously determined by single-crystal X-ray diffraction (SCXRD) analysis, electrospray ionization mass spectrometry (ESI-MS), and Fourier-transform infrared spectroscopy (FTIR). The formation of the **EuNTA** complex was also confirmed by nuclear magnetic resonance spectroscopy (NMR). The ^{1}H NMR spectrum of **EuNTA** shows only a single set of resonance signals, implying that a discrete species exists in solution (Fig. 2a and Fig. S1 in the SI), and the peaks were further verified using 2D COSY spectra (Fig. S2). Compared with the NTA ligand, the **EuNTA** complex displayed broader signals due to the paramagnetic nature of the Eu(III) ion.[44,45] Meanwhile, the protons in the ligand moiety all shifted to the high-field region after coordination (Fig. 2b). The hydroxy H^a on the β-diketone group of **EuNTA** disappeared at 15.2 ppm, indicating the successful coordination of Eu(III) with the NTA ligand. Considering the strong coordination capability of diketone with Ln(III), **LnNTA** could be stable for ESI-MS characterization. As shown in the negative mode ESI-MS results (Fig. 2b), for **EuNTA**, a singly charged peak at m/z = 1211.11 was found, which is in agreement with the theoretical molecular weight of 1211.11 Da. The formation and purity of other four LnNTA complexes were confirmed by ESI-MS (Fig. S3–S6) and FTIR (Fig. S7).

Colorless plate crystals of **LnNTA** with five different Ln metals suitable for single-crystal X-ray diffraction were obtained by slow vaporization of **LnNTA** in a solution of methanol and dichloromethane (1 : 1, v/v); they are isostructural and crystallize as monoclinic crystals with a chiral space group of $P2_1$ (Fig. 3 and Fig. S8). Here, we have taken **EuNTA** as an example to analyze its structure. As illustrated in Fig. 3a, there are four NTA anions, one positive Eu(III) ion, and one TEA cation in the dissymmetric unit. The anionic NTA chelates to the central Eu(III) ion *via* the ketone functional groups, leading to the formation of a six-membered ring. In the complex, the Eu(III) anion is eight-coordinated by the oxygen donor atoms of four NTA anions. The bond lengths of Eu–O are in the range of 2.335(4) to 2.442(3) Å. The distance between the TEA cation and the Eu(III) ion is 5.735(3) Å.

The chiral space group $P2_1$ of **EuNTA** confirms the spontaneous resolution during crystallization. Then, we carefully compared the chiral feature in single molecules and the packing modes. The two enantiomers are distinguished by the helicity of the arrangement between the left-handed (Λ) and the right-handed (Δ) helical isomers through enantioseparation (Fig. 1b). Similarly, for the octahedral coordination sphere of the central metal ion with bichelated β-diketonato ligands, if one ligand was chosen as an axis, other three ligands also located in a spatial arrangement, showing a Λ configuration (left-handed spiral) or a Δ configuration (right-handed spiral). For the **EuNTA** complex, Λ and Δ configurations can be easily recognized, as shown in Fig. 1 and 3. Both **Λ-LnNTA** and **Δ-LnNTA** enantiomers occur within a single crystallization batch. The Λ- and Δ-enantiomers were unequivocally characterized by SCXRD analysis, as they were indistinguishable by macroscopic observation.

To understand the driving force behind such spontaneous resolution or the chiral self-sorting process, intermolecular packing interactions in **EuNTA** were examined. First, strong π–π interactions (3.67–3.84 Å) of the naphthyl groups of nearby **EuNTA** molecules were found along the *b* axis, resulting in one-dimensional (1D) chains (Fig. 3b). Second, five C–H···π interactions ranging from 2.59 to 3.11 Å among the TEA cation and three naphthyl groups of different **EuNTA** molecules on the *bc* plane could be observed (Fig. 3c). Upon the cooperation effect of these π–π and C–H···π interactions, the homochiral **EuNTA** molecules tended to achieve two-dimensional (2D) layers. Third, the weak intermolecular C–H···F interactions further assembled the abovementioned 2D layers into homochiral three-dimensional (3D) conglomerates rather than a racemic assembly (Fig. 3c and Fig. S9, S10). As such, the Λ and Δ configurations can be separated into homochiral **Λ-EuNTA** and **Δ-EuNTA** single crystals (Fig. 3e and f) with spontaneous resolution.

In addition to chiral structure analysis, the photophysical properties of racemic **EuNTA** complex crystals were explored. First, **EuNTA** possesses maximal absorption at 332 nm, which is attributed to the NTA ligand, with a molar extinction coefficient (ε) as high as 88 500 M^{-1} cm^{-1} (Fig. S11), superior to those of conventional chiral Eu(III) complexes (Fig. 1a).[32,33] As illustrated in Fig. S12, the **EuNTA** complex emits red luminescence at 614 nm upon excitation at 326 nm in solution. The emission spectrum displays characteristic peaks at 593, 614, 652, and 700 nm, assigned to the $^5D_0 \rightarrow {}^7F_J$ (J = 1–4) transitions of Eu^{3+}. The markedly enhanced intensity of the 614 nm peak ($^5D_0 \rightarrow {}^7F_2$) indicates a dominant electric dipole character, confirming the low symmetry of the Eu^{3+} coordi-

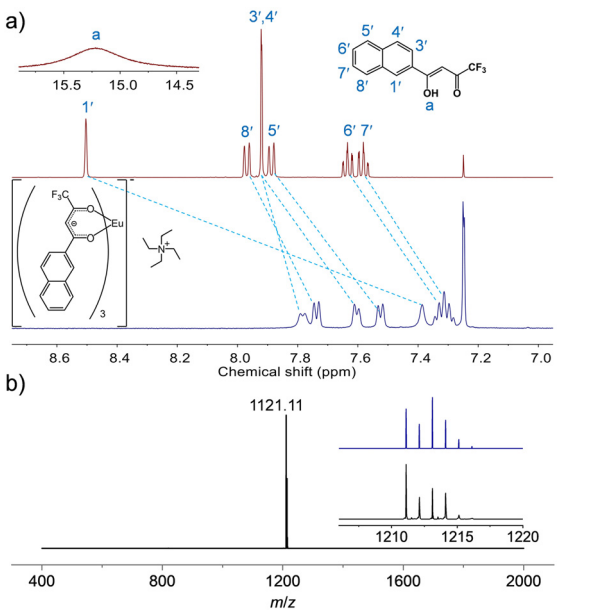

Fig. 2 Characterization of **EuNTA**. (a) ^{1}H NMR spectra of the NTA ligand and **EuNTA** complex in $CDCl_3$. (b) ESI-MS spectrum of the **EuNTA** complex. Note: the blue ones are the theoretical peaks.

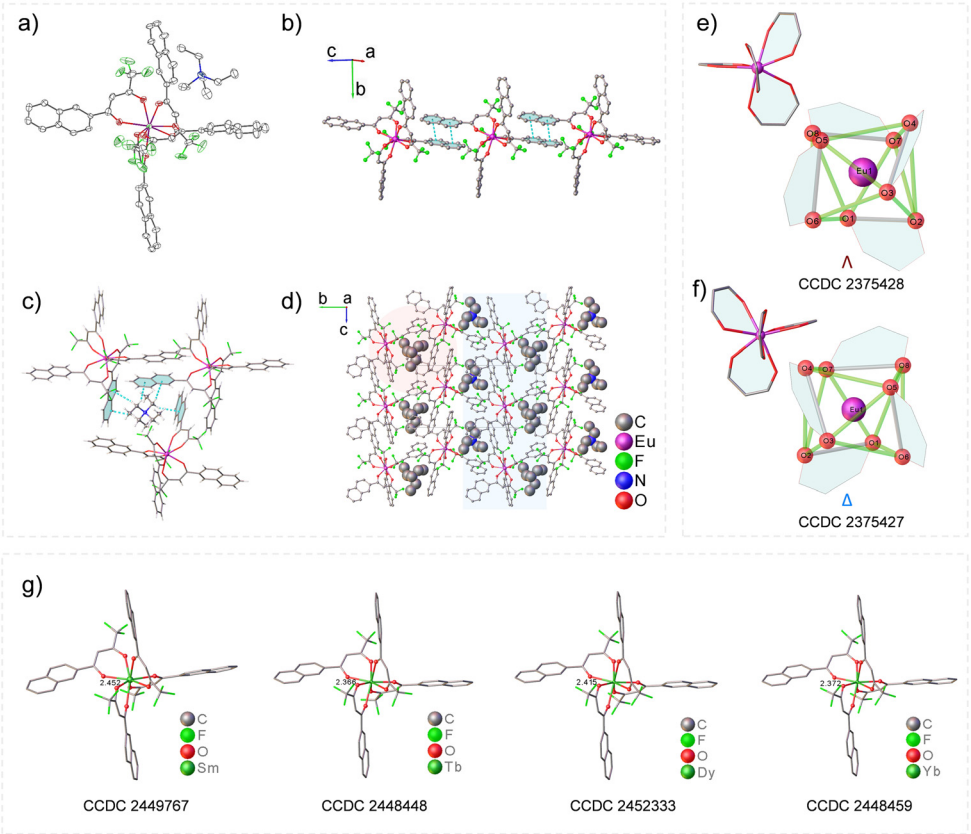

Fig. 3 Crystallization-induced homochiral **Λ-EuNTA** or **Δ-EuNTA**. (a) The asymmetric unit of the **EuNTA** complex. (b) The π–π interaction of naphthalene groups in the nearby complex. Hydrogen atoms are omitted for clarity. (c) The C–H···π interaction of the TEA cation with naphthalene groups in the **EuNTA** complex. (d) The 3D packing of the **EuNTA** complex along the *a* axis. (e and f) β-diketone planes of NTA anions and coordination geometry of Eu(III) centers in **Λ-EuNTA** and **Δ-EuNTA**, respectively. (g) Crystal structures of **Δ-SmNTA**, **Δ-TbNTA**, **Δ-DyNTA**, and **Δ-YbNTA**.

nation environment. This conclusion is fully consistent with our crystallographic analysis. Remarkably, this luminescence at 614 nm has a narrow FWHM of *ca.* 5 nm in solution (dichloromethane, 1×10^{-5} M) with a lifetime of 532 μs (Fig. S13), fulfilling the requirement of high color purity. Because solution samples consume massive chemicals, thus compromising their operation, solid thin films are more desirable.[46,47] A KBr thin pellet containing 0.5% w/w of EuNTA complex (thickness: 0.5 mm) was obtained through grinding and tablet pressing and it exhibits an FWHM of 5 nm, resulting in ultra-narrowband luminescence in the solid state (Fig. 4a). Beyond narrowband luminescence, the quantum yield (QY) of luminescence is another crucial parameter to evaluate luminescent materials. While in the pursuit of narrowband luminescence through chiral ligand–lanthanide complexing, the luminescence QY was suppressed in many cases.[32] Due to the superb light harvesting efficiency of the aromatic structure 1-(2-naphthoyl)-3,3,3-trifluoroacetone, the thin pellet of **EuNTA** gives a QY of 91% (Fig. S14), acting as a bright CPL thin film. Finally, the luminescence decay of **EuNTA** was calculated. The luminescence lifetime of **EuNTA** at 614 nm was 282 μs upon excitation at 326 nm, which is in agreement with that of regular Eu(III) complexes.[21,48]

Given the specific chiral property originating from chiral separation, the chiroptical activities of **Λ-EuNTA** or **Δ-EuNTA** of the homochiral single crystals were investigated by circular dichroism (CD) and circularly polarized luminescence (CPL). Enantiomerically pure samples were obtained by manual separation guided by absolute configuration determination *via* SCXRD. For CPL characterization, the isolated enantiomers were homogenized with KBr using an agate mortar and subsequently pressed into 0.5 mm thick pellets containing precisely 0.5% w/w of either the **Λ-EuNTA** or **Δ-EuNTA** complex. In the CD measurement, we could observe opposite signals for this pair of enantiomers (Fig. S15), indicative of the optical chirality in the ground state. Since the measurements were performed on solid samples, we observed characteristic spectral distortions and red shifts in the solid-state CD spectra, which are attributable to concentration effects in the thin film state.[49–51] Meanwhile, as a descriptor of excited-state chirality, CPL can be used to evaluate the macroscopic chirality of chiral materials. The primary criterion for assessing CPL is to calculate the luminescence dissymmetry factor, $g_{lum} = 2(I_L - I_R)/(I_L + I_R)$, which provides the luminescence difference of left-handed (L) and right-handed (R) circularly polarized light. As illustrated in Fig. 4c, after exposure to 326 nm excitation, the

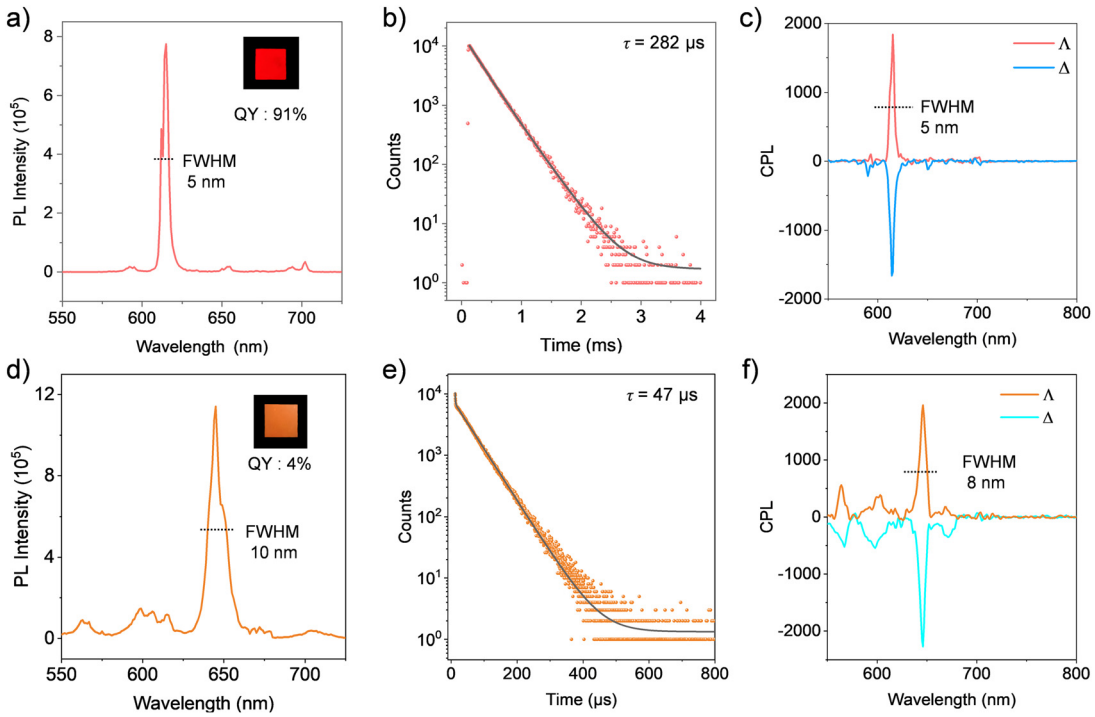

Fig. 4 Regular and chiral luminescence properties. (a and d) Luminescence spectra of **EuNTA** and **SmNTA** complexes and (b and e) luminescence decay curves of **EuNTA** and **SmNTA** in the thin film at room temperature (λ_{ex} = 326 nm and 380 nm), respectively. (c and f) CPL spectra of **Λ-EuNTA**, **Δ-EuNTA**, **Λ-SmNTA**, and **Δ-SmNTA** in the thin film state at room temperature, respectively.

Λ-EuNTA or **Δ-EuNTA** thin pellet produced positive or negative CPL with a sharp peak at 614 nm. Both films with two enantiomers were observed with $|g_{lum}|$ values of ~0.02, which falls within the typical range (10^{-3}–10^{-1}) reported for Eu(III) complexes emitting at around 614 nm.[21–29] Moreover, in contrast to decreasing CPL resulting from the racemization in solution (Fig. S16 and S17),[52] such thin pellets of **Λ-EuNTA** and **Δ-EuNTA** exhibit a relatively stable chiroptical activity (Fig. S18). These CPL results further demonstrate the unique feature of crystal engineering-induced chiral separation of **EuNTA**. Similar to regular luminescence, the CPL of **Λ-EuNTA** and **Δ-EuNTA** has a remarkably narrow FWHM of 5 nm, which completely agrees with that of regular luminescence, indicating the consistence between regular and circularly polarized luminescence. To the best of our knowledge, the FWHM of **Λ-EuNTA** and **Δ-EuNTA** is among the smallest ones for organic and inorganic CPL materials.[33,52] To systematically evaluate the CPL stability of **EuNTA** chiral crystals, we conducted measurements over a three-week period (testing at 1 week, 2 week, and 3 week intervals) under identical experimental conditions (Fig. S18). The results demonstrate good stability, with the CPL intensity of the film sample showing negligible degradation (<5%) throughout the testing period. These results show that the physical properties and luminescence of chiral crystals are very stable, and it shows their good potential for advanced luminescence applications, which warrants further exploration.

Given the notable luminescence properties of lanthanides, we extended our investigation to Sm(III), Tb(III), and Dy(III) complexes. The **SmNTA** complex exhibits characteristic emission peaks at 563, 598, 645, and 705 nm, corresponding to the $^4G_{5/2} \rightarrow {}^6H_{5/2}$, $^6H_{7/2}$, $^6H_{9/2}$, and $^6H_{11/2}$ transitions of Sm^{3+}, respectively (Fig. 4d and Fig. S20). The most intense transition ($^4G_{5/2} \rightarrow {}^6H_{9/2}$) displays a narrow FWHM of 10 nm and a lifetime of 47 μs (Fig. 4e), with a quantum yield of 4% (Fig. S21). These results indicate that the NTA ligand serves as a significantly more efficient antenna for Eu(III) than for Sm(III). Notably, the **TbNTA** and **DyNTA** complexes show no detectable lanthanide-centered emission, instead exhibiting only ligand-based luminescence at 476 nm and 499 nm, respectively (Fig. S22 and S23). This dramatic variation in luminescence behavior across the lanthanide series can be understood by considering the energy level matching between the ligand's triplet state (T_1) and the lanthanide's excited states. The T_1 energy level of the ligand should be approximately 2000–4000 cm^{-1} higher than the excited state of the rare-earth ion (empirical value). For Eu^{3+}, the $^5D_0$ energy level (17 200 cm^{-1}) is well matched with NTA's T_1 energy of 20 000 cm^{-1},[53,54] falling within the optimal range of 19 000–21 000 cm^{-1}. In contrast, for Tb^{3+}, whose $^5D_4$ energy level (20 500 cm^{-1}) requires a ligand with $T_1 \geq 22\,500$ cm^{-1}, the NTA ligand proves inadequate for efficient energy transfer, explaining the observed ligand-dominated luminescence. CPL measurements were performed on KBr pellets containing SCXRD-verified **Λ-SmNTA** or **Δ-SmNTA** enantiomers. Mirroring the behavior of **EuNTA**, both **Λ-SmNTA** and **Δ-SmNTA** enantiomers exhibit remarkably narrow CPL bands

(FWHM = 8 nm), which peaked at 645 nm with $|g_{lum}|$ values of approximately 0.006 (Fig. 4f).

Conclusions

CPL is a high-level visual perception for supplying one more dimension of information compared to regular luminescence, and it has attracted much attention over the past 10 years and is now at the frontier of physics, chemistry and materials science. Beyond luminescence dissymmetry and strong emission, the color purity (narrowband emission) of CPL has been ignored in the long term. Making full use of the narrowband emission property of metal–organic Eu(III) complexes, we have developed rare earth complexes **Λ-EuNTA** and **Δ-EuNTA** with ultra-narrowband CPL with a FWHM of 5 nm at 614 nm, accompanied by a lifetime of 282 μs. To improve the emission efficiency of chiral Eu(III) complexes, we employed the π-conjugated ligand 1-(2-naphthoyl)-3,3,3-trifluoroacetone to enhance the light harvesting ability, resulting in highly emissive luminescence (QY: 91%). By symmetry breaking and spontaneous resolution, high-dissymmetry CPL with a $|g_{lum}|$ value of ∼0.02 was achieved. Taken together, our strategy could solve well the circularly polarized luminescence dilemma between high dissymmetry and strong emission. We have thus achieved narrowband-luminescence, persistent and highly emissive CPL, with potential for use in pure color displays.

Data availability

The data supporting this article have been included as part of the SI. It contains materials, characterization methods, synthetic protocols, crystallographic data tables, bonds length tables, ^{1}H NMR, COSY, ESI-MS, IR, UV-vis, luminescence, CD, CPL spectra, and crystal structure figures of **LnNTA** complexes. See DOI: **https://doi.org/10.1039/d5qi01288k**.

CCDC 2448433, 2449767, 2375427, 2375428, 2449819, 2448448, 2448434, 2452333, 2449766 and 2448459 contain the supplementary crystallographic data for this paper.[55a–j]

Author contributions

Z. C., Y. W., and W.-H. Z. designed and conceived the experiments; Z. C., W. X., C. H., Z. L., S. L., M. H., and S. G. performed the experiments and analysed the data; Z. C., W. X., Z.-Q. Y., and Y. W. wrote the paper; all authors contributed to the general discussion.

Conflicts of interest

There are no conflicts to declare.

Acknowledgements

We acknowledge the support from the Basic Science Center of National Natural Science Foundation (T2488302), the National Natural Science Foundation of China (92356301), the Guangdong Basic and Applied Basic Research Foundation (2024A1515030126), the Innovation Research Foundation of Shenzhen (20231120172320001), the Guangdong Province "Pearl River Talents Plan" Innovative and Entrepreneurial Teams Project (2021ZT09C289), and the Scientific Foundation for Youth Scholars of Shenzhen University (868-000001032092 and 868-000001032093). We also greatly appreciate the helpful discussion with Prof. Xiaopeng Li from Shenzhen University. We thank the Instrumental Analysis Center of Shenzhen University for the usage of the SCXRD instrument.

References

1 M. Liu, L. Zhang and T. Wang, Supramolecular chirality in self-assembled systems, *Chem. Rev.*, 2015, **115**, 7304–7397.
2 Y. Wu, M. Li, Z.-G. Zheng, Z.-Q. Yu and W.-H. Zhu, Liquid crystal assembly for ultra-dissymmetric circularly polarized luminescence and beyond, *J. Am. Chem. Soc.*, 2023, **145**, 12951–12966.
3 X. Yang, X. Gao, Y.-X. Zheng, H. Kuang, C.-F. Chen, M. Liu, P. Duan and Z. Tang, Recent progress of circularly polarized luminescence materials from chinese perspectives, *CCS Chem.*, 2023, **5**, 2760–2789.
4 X. Lu, K. Zhang, X. Niu, D.-D. Ren, Z. Zhou, L.-L. Dang, H.-R. Fu, C. Tan, L. Ma and S.-Q. Zang, Encapsulation engineering of porous crystalline frameworks for delayed luminescence and circularly polarized luminescence, *Chem. Soc. Rev.*, 2024, **53**, 6694–6734.
5 D.-W. Zhang, M. Li and C.-F. Chen, Recent advances in circularly polarized electroluminescence based on organic light-emitting diodes, *Chem. Soc. Rev.*, 2020, **49**, 1331–1343.
6 J. R. Brandt, F. Salerno and M. J. Fuchter, The added value of small-molecule chirality in technological applications, *Nat. Rev. Chem.*, 2017, **1**, 0045.
7 M. Cao, Y. Ren, Y. Wu, J. Shen, S. Li, Z.-Q. Yu, S. Liu, J. Li, O. J. Rojas and Z. Chen, Biobased and biodegradable films exhibiting circularly polarized room temperature phosphorescence, *Nat. Commun.*, 2024, **15**, 2375.
8 Y. Wu, C. Yan, X.-S. Li, L.-H. You, Z. Q. Yu, X. Wu, Z. Zheng, G. Liu, Z. Guo, H. Tian and W.-H. Zhu, Circularly polarized fluorescence resonance energy transfer (*C*-FRET) for efficient chirality transmission within an intermolecular system, *Angew. Chem., Int. Ed.*, 2021, **60**, 24549–24557.
9 Y. Wu, Y. Ren, X. Zeng, H. Hu, M. Li, J. Li, T. He, X. S. Li, Z. Q. Yu and W. H. Zhu, Enhancing tetraphenylethene cyclization as photoswitch, *Smart Mol.*, 2023, **1**, e20230003.
10 T. He, C. Ren, Y. Luo, Q. Wang, J. Li, X. Lin, C. Ye, W. Hu and J. Zhang, Water-soluble chiral tetrazine derivatives: Towards the application of circularly polarized lumine-

scence from upper-excited states to photodynamic therapy, *Chem. Sci.*, 2019, **10**, 4163–4168.
11 Parameter values for ultra-high definition television systems for production and international programme exchange, 2012, ITU-R BT.2020, https://www.itu.int/rec/r-rec-bt.2020/en.
12 S. E. Penty, G. R. F. Orton, D. J. Black, R. Pal, M. A. Zwijnenburg and T. A. Barendt, A chirally locked bisperylene diimide macrocycle: Consequences for chiral self-assembly and circularly polarized luminescence, *J. Am. Chem. Soc.*, 2024, **146**, 5470–5479.
13 X. Zou, N. Gan, M. Dong, W. Huo, A. Lv, X. Yao, C. Yin, Z. Wang, Y. Zhang, H. Chen, H. Ma, L. Gu, Z. An and W. Huang, Narrowband organic afterglow via phosphorescence Förster resonance energy transfer for multifunctional applications, *Adv. Mater.*, 2023, **35**, 2210489.
14 Y. Liu, Z. Ma, Z. Wang and W. Jiang, Boosting circularly polarized luminescence performance by a double π-helix and heteroannulation, *J. Am. Chem. Soc.*, 2022, **144**, 11397–11404.
15 H. Gao, Y. Liu, W. Lian, P. Hu, X. Shang, M. Chen, X. Song, T. Guan and X. Chen, Near-infrared circularly polarized light triggered phototherapy based on hybrid $CuInSe_2$ quantum dot hydrogels, *Nano Today*, 2024, **58**, 102436.
16 D. Serrano, S. K. Kuppusamy, B. Heinrich, O. Fuhr, D. Hunger, M. Ruben and P. Goldner, Ultra-narrow optical linewidths in rare-earth molecular crystals, *Nature*, 2022, **603**, 241–246.
17 S. Schlittenhardt, E. Vasilenko, V. Unni C., N. Jobbitt, O. Fuhr, D. Hunger, M. Ruben and S. K. Kuppusamy, Spectral hole–burning studies of a mononuclear Eu(III) complex reveal narrow optical linewidths of the $^5D_0 \rightarrow {}^7F_0$ transition and seconds long nuclear spin lifetimes, *ChemPhysChem*, 2024, **25**, e202400280.
18 S. K. Kuppusamy, E. Vasilenko, W. Li, J. Hessenauer, C. Ioannou, O. Fuhr, D. Hunger and M. Ruben, Observation of narrow optical homogeneous linewidth and long nuclear spin lifetimes in a prototypical [Eu(trensal)] complex, *J. Phys. Chem. C*, 2023, **127**, 10670–10679.
19 X.-Z. Li, L.-P. Zhou, L.-L. Yan, D.-Q. Yuan, C.-S. Lin and Q.-F. Sun, Evolution of luminescent supramolecular lanthanide $M_{2n}L_{3n}$ complexes from helicates and tetrahedra to cubes, *J. Am. Chem. Soc.*, 2017, **139**, 8237–8244.
20 P.-R. Su, T. Wang, P.-P. Zhou, X.-X. Yang, X.-X. Feng, M.-N. Zhang, L.-J. Liang, Y. Tang and C.-H. Yan, Self-assembly-induced luminescence of Eu^{3+}-complexes and application in bioimaging, *Natl. Sci. Rev.*, 2022, **9**, nwab016.
21 L. Llanos, P. Cancino, P. Mella, P. Fuentealba and D. Aravena, Circularly polarized luminescence and coordination geometries in mononuclear lanthanide(III) complexes, *Coord. Chem. Rev.*, 2024, **505**, 215675.
22 N. Liang, C. Cao, Z. Xie, J. Liu, Y. Feng and C.-J. Yao, Advances in near-infrared circularly polarized luminescence with organometallic and small organic molecules, *Mater. Today*, 2024, **75**, 309–333.
23 Y. Zhong, Z. Wu, Y. Zhang, B. Dong and X. Bai, Circularly polarized luminescence of lanthanide complexes: From isolated individuals, discrete oligomers, to hierarchical assemblies, *InfoMat*, 2022, **5**, 12392.
24 Y. Zhang, S. Yu, B. Han, Y. Zhou, X. Zhang, X. Gao and Z. Tang, Circularly polarized luminescence in chiral materials, *Matter*, 2022, **5**, 837–875.
25 L. E. MacKenzie and R. Pal, Circularly polarized lanthanide luminescence for advanced security inks, *Nat. Rev. Chem.*, 2020, **5**, 109–124.
26 H.-Y. Wong, W.-S. Lo, K.-H. Yim and G.-L. Law, Chirality and chiroptics of lanthanide molecular and supramolecular assemblies, *Chem*, 2019, **5**, 3058–3095.
27 R. Carr, N. H. Evans and D. Parker, Lanthanide complexes as chiral probes exploiting circularly polarized luminescence, *Chem. Soc. Rev.*, 2012, **41**, 7673–7686.
28 D. Parker, R. S. Dickins, H. Puschmann, C. Crossland and J. A. K. Howard, Being excited by lanthanide coordination complexes: aqua species, chirality, excited-state chemistry, and exchange dynamics, *Chem. Rev.*, 2002, **102**, 1977–2010.
29 S. Petoud, G. Muller, E. G. Moore, J. Xu, J. Sokolnicki, J. P. Riehl, U. N. Le, S. M. Cohen and K. N. Raymond, Brilliant Sm, Eu, Tb, and Dy chiral lanthanide complexes with strong circularly polarized luminescence, *J. Am. Chem. Soc.*, 2007, **129**, 77–83.
30 J. L. Lunkley, D. Shirotani, K. Yamanari, S. Kaizaki and G. Muller, Extraordinary circularly polarized luminescence activity exhibited by cesium tetrakis(3-heptafluoro-butylryl-(+)-camphorato) Eu(III) complexes in EtOH and $CHCl_3$ solutions, *J. Am. Chem. Soc.*, 2008, **130**, 13814–13815.
31 J. L. Lunkley, D. Shirotani, K. Yamanari, S. Kaizaki and G. Muller, Chiroptical spectra of a series of tetrakis((+)-3-heptafluorobutylyrylcamphorato)lanthanide(III) with an encapsulated alkali metal ion: circularly polarized luminescence and absolute chiral structures for the Eu(III) and Sm(III) complexes, *Inorg. Chem.*, 2011, **50**, 12724–12732.
32 T. Harada, H. Tsumatori, K. Nishiyama, J. Yuasa, Y. Hasegawa and T. Kawai, Nona-coordinated chiral Eu(III) complexes with stereoselective ligand–ligand noncovalent interactions for enhanced circularly polarized luminescence, *Inorg. Chem.*, 2012, **51**, 6476–6485.
33 M. Tsurui, R. Takizawa, Y. Kitagawa, M. Wang, M. Kobayashi, T. Taketsugu and Y. Hasegawa, Chiral tetrakis Eu(III) complexes with ammonium cations for improved circularly polarized luminescence, *Angew. Chem., Int. Ed.*, 2024, **63**, e202405584.
34 Z.-F. Liu, X.-Y. Ye, L. Chen, L.-Y. Niu, W. J. Jin, S. Zhang and Q.-Z. Yang, Spontaneous symmetry breaking of achiral molecules leading to the formation of homochiral superstructures that exhibit mechanoluminescence, *Angew. Chem., Int. Ed.*, 2024, **63**, e202318856.
35 Y. Chen, J. Zhang, J. Zhang and X. Wan, Directional crystal jumping controlled by chirality, *J. Am. Chem. Soc.*, 2024, **146**, 9679–9687.

36 C. Xu, Q. Lin, C. Shan, X. Han, H. Wang, H. Wang, W. Zhang, Z. Chen, C. Guo, Y. Xie, X. Yu, B. Song, H. Song, L. Wojtas and X. Li, Metallo–supramolecular octahedral cages with three types of chirality towards spontaneous resolution, *Angew. Chem., Int. Ed.*, 2022, **61**, e202203099.

37 X. Lin, B. Kou, J. Cao, P. Weng, X. Yan, Z. Li and Y.-B. Jiang, Spontaneous resolution of helical building blocks through the formation of homochiral helices in two dimensions, *Angew. Chem., Int. Ed.*, 2022, **61**, e202205914.

38 P. M. Burrezo, V. G. Jiménez, D. Blasi, I. Ratera, A. G. Campaña and J. Veciana, Organic free radicals as circularly polarized luminescence emitters, *Angew. Chem., Int. Ed.*, 2019, **58**, 16282–16288.

39 J. Kim, J. Lee, W. Y. Kim, H. Kim, S. Lee, H. C. Lee, Y. S. Lee, M. Seo and S. Y. Kim, Induction and control of supramolecular chirality by light in self-assembled helical nanostructures, *Nat. Commun.*, 2015, **6**, 6959.

40 F. R. Fronczek, A. K. Banerjee, S. F. Watkins and R. W. Schwartz, Absolute configuration and circular dichroism of the lanthanide complex: Trisodiumtris(oxydiacetato) europate(III) bis(sodium tetrafluoroborate) hexahydrate, *Inorg. Chem.*, 1981, **20**, 2745–2746.

41 K. Binnemans, Lanthanide-based luminescent hybrid materials, *Chem. Rev.*, 2009, **109**, 4283–4374.

42 S. M. Bruno, R. A. S. Ferreira, F. A. A. Paz, L. D. Carlos, M. Pillinger, P. Ribeiro-Claro and I. S. Gonçalves, Structural and photoluminescence studies of a europium(III) tetrakis (β-diketonate) complex with tetrabutylammonium, imidazolium, pyridinium and silica-supported imidazolium counterions, *Inorg. Chem.*, 2009, **48**, 4882–4895.

43 F. A. Mautner, F. Bierbaumer, M. Gyurkac, R. C. Fischer, A. Torvisco, S. S. Massoud and R. Vicente, Synthesis and characterization of lanthanum(III) complexes containing 4,4,4-trifluoro-1-(naphthalen-2yl)butane-1,3-dionate, *Polyhedron*, 2020, **179**, 114384.

44 D. F. Caffrey, T. Gorai, B. Rawson, M. Martínez-Calvo, J. A. Kitchen, N. S. Murray, O. Kotova, S. Comby, R. D. Peacock, P. Stachelek, R. Pal and T. Gunnlaugsson, Ligand chirality transfer from solution state to the crystalline self-assemblies in circularly polarized luminescence (CPL) active lanthanide systems, *Adv. Sci.*, 2024, **11**, 2307448.

45 M. Li, Y. Zhou, Y. Yao, T. Gao, P. Yan and H. Li, Designing water-quenching resistant highly luminescent europium complexes by regulating the orthogonal arrangement of bis-β-diketone ligands, *Dalton Trans.*, 2021, **50**, 9914–9922.

46 J. Han, Y. Shi, X. Jin, X. Yang and P. Duan, Regulating the excited state chirality to fabricate high-performance-solid-state circularly polarized luminescence materials, *Chem. Sci.*, 2022, **13**, 6074–6080.

47 X. Pan, L. Lan and H. Zhang, Flexible organic crystals with multi-stimuli-responsive CPL for broadband multicolor optical waveguides, *Chem. Sci.*, 2024, **15**, 17444–17452.

48 S. E. Bodman and S. J. Butler, Advances in anion binding and sensing using luminescent lanthanide complexes, *Chem. Sci.*, 2021, **12**, 2716–2734.

49 H. Zhang, J.-X. Yan, S.-T. Wu, D. Li, S.-G. Wan, L. Ding and L.-R. Lin, Further understanding on the measurement methods for solid-state circular dichroism spectroscopy - discussion on concentration effects, *Acta Phys. Chim. Sin.*, 2013, **29**, 2481–2497.

50 Y. Lin, F. Zou, S. Wan, J. Ouyang, L. Lin and H. Zhang, Dynamic chiral-at-metal stability of tetrakis(D/L-hfc)Ln(III) complexes capped with an alkali metal cation in solution, *Dalton Trans.*, 2012, **41**, 6696–6706.

51 Q.-X. Yao, W.-M. Xuan, H. Zhang, C.-Y. Tu and J. Zhang, The formation of a hydrated homochiral helix from an achiral zwitterionic salt, spontaneous chiral symmetry breaking and redox chromism of crystals, *Chem. Commun.*, 2009, **1**, 59–61.

52 Y. Ren, Z. Chen, H. Hu, Z. Zhang, B. Yang, Z. Zheng, Z.-Q. Yu, X. Li, W.-H. Zhu and Y. Wu, FRET endows rare earth Eu(III) complex with stable ultra-dissymmetry and narrowband circularly polarized luminescence, *Sci. China Mater.*, 2024, **68**, 879–887.

53 S. Dasari, S. Singh, S. Sivakumar and A. K. Patra, Dual-sensitized luminescent europium(iotaiotaiota) and terbium (iotaiotaiota) complexes as bioimaging and light-responsive therapeutic agents, *Chem. – Eur. J.*, 2016, **22**, 17387–17396.

54 I. V. Taydakov, A. A. Akkuzina, R. I. Avetisov, A. V. Khomyakov, R. R. Saifutyarov and I. C. Avetissov, Effective electroluminescent materials for OLED applications based on lanthanide 1.3-diketonates bearing pyrazole moiety, *J. Lumin.*, 2016, **177**, 31–39.

55 (*a*) W. Xu, CCDC 2448433 (**Λ-SmNTA**): Experimental Crystal Structure Determination, 2025, DOI: **10.5517/ccdc.csd.cc2n5sqc**; (*b*) W. Xu, CCDC 2449796 (**Λ-EuNTA**): Experimental Crystal Structure Determination, 2025, DOI: **10.5517/ccdc.csd.cc2n76pt**; (*c*) W. Xu, CCDC 2375427 (**Λ-TbNTA**): Experimental Crystal Structure Determination, 2025, DOI: **10.5517/ccdc.csd.cc2kqtpt**; (*d*) W. Xu, CCDC 2375428 (**Λ-DyNTA**): Experimental Crystal Structure Determination, 2025, DOI: **10.5517/ccdc.csd.cc2kqtqv**; (*e*) W. Xu, CCDC 2449819 (**Λ-YbNTA**): Experimental Crystal Structure Determination, 2025, DOI: **10.5517/ccdc.csd.cc2n77fl**; (*f*) W. Xu, CCDC 2448448 (**Δ-SmNTA**): Experimental Crystal Structure Determination, 2025, DOI: **10.5517/ccdc.csd.cc2n5t6w**; (*g*) W. Xu, CCDC 2448434 (**Δ-EuNTA**): Experimental Crystal Structure Determination, 2025, DOI: **10.5517/ccdc.csd.cc2n5srd**; (*h*) W. Xu, CCDC 2452333 (**Δ-TbNTA**): Experimental Crystal Structure Determination, 2025, DOI: **10.5517/ccdc.csd.cc2n9vjc**; (*i*) W. Xu, CCDC 2449766 (**Δ-DyNTA**): Experimental Crystal Structure Determination, 2025, DOI: **10.5517/ccdc.csd.cc2n75qt**; (*j*) W. Xu, CCDC 2448459 (**Δ-YbNTA**): Experimental Crystal Structure Determination, 2025, DOI: **10.5517/ccdc.csd.cc2n5tk7**.